Nernst coefficient within relaxation time approximation

Mona Zebarjadi, S. Emad Rezaei, Md Sabbir Akhanda, and Keivan Esfarjani

Nernst Coefficient within relaxation time approximation

Mona Zebarjadi[a,b], Emad Rezaei[a], Sabbir Akhanda[a], Keivan Esfarjani[b,c,d]

[a] *Department of Electrical and Computer Engineering, University of Virginia, Charlottesville,*

Virginia 22904, USA

[b] *Department of Materials Science and Engineering, University of Virginia, Charlottesville,*

Virginia 22904, USA

[c] *Department of Mechanical and Aerospace Engineering, University of Virginia, Charlottesville,*

Virginia 22904, USA

[d] *Department of Physics, University of Virginia, Charlottesville, Virginia 22904, USA*

1. Abstract

Analytical solutions based on the Boltzmann transport equation (BTE) within the relaxation time approximation are developed to relate the Nernst coefficient to materials band structure and relaxation times parameters in simple conductors. The dependence of the Nernst coefficient on the effective mass, anisotropy of bands, energy bandgap, and scattering parameters are investigated. The obtained relations are compared to the existing solutions presented in the past using different approximations.

2. Introduction:

Thermomagnetic energy conversion based on the Nernst effect and thermomagnetic refrigeration based on the Ettingshausen cooling provides a solid-state technique for direct conversion of heat to electricity and pumping of heat from the cold reservoir to the hot one. Thermomagnetic modules are similar to thermoelectric modules (see Fig. 1). A temperature gradient applied to a conductor results in a longitudinal Seebeck voltage which is the base of the thermoelectric heat to electricity, energy conversion. When a magnetic field is applied normal to the imposed temperature

gradient, there will be a secondary transverse voltage, the so-called Nernst voltage. [1] The Nernst coefficient, N, is then defined as the transverse voltage gradient divided by the temperature gradient (we do not divide by the magnetic field and assume N is in the units of V/K), has the same dimensions as the Seebeck coefficient, and is the base of the thermomagnetic energy conversion. (Figure 1).

$$\alpha = -\frac{\Delta V}{\Delta T}$$

$$\overrightarrow{E_N} = N\,\vec{B} \times \overrightarrow{VT}$$

Figure 1. Schematic of the a)Seebeck effect b) Nernst effect c) Thermoelectric module for refrigeration d) Thermomagnetic modules for refrigeration.

The thermomagnetic efficiency of materials for power generation and refrigeration applications is evaluated by their dimensionless figure of merit, $z_{TM}T$ defined as $(N^2\sigma_{yy}T)/\kappa_{xx}$ where σ_{yy} is the electrical conductivity in the y-direction (direction of the Nernst voltage), κ_{xx} is the thermal conductivity along the direction of the applied thermal gradient, and T is the average temperature of the material [2]. Historically, the Nernst coefficient was first observed in Bismuth in 1886. [1] It was then measured in many metals [3–7] semimetals [8–11] and narrow-gap semiconductors [12–15]. Previous studies have shown that extremely mobile quasi-particles in dilute metals generate a noticeable Nernst signal. [16] Within the Fermi liquid picture, it is shown that the Nernst effect roughly measures the ratio of electron mobility to Fermi energy in a given metal. [17,18]

In addition to power generation and cooling, the Nernst effect has been used as an experimental probe in studying various physical systems, for instance, in determining the carrier-scattering mechanisms involved in semiconductors and semimetals [14,19–22].

The theory of the Seebeck coefficient is well developed and the analytical solutions for the Seebeck coefficient are well known. For instance, we know that the Seebeck coefficient, α, in metals follow Mott's formula and is an increasing function of the derivative of the logarithm of the electrical conductivity, σ, with respect to energy, ε, at the Fermi energy, ε_f ($\alpha = \frac{\pi^2 k_B^2 T}{3q}\frac{d\log(\sigma)}{d\varepsilon}\big|_{\varepsilon_f}$ where k_B is the Boltzmann constant, T is the temperature, and $e = 1.6 \times 10^{-19} C$ is the unit of charge). This suggests that materials with a large slope of the density of states and relaxation times with respect to energy own a large Seebeck coefficient.
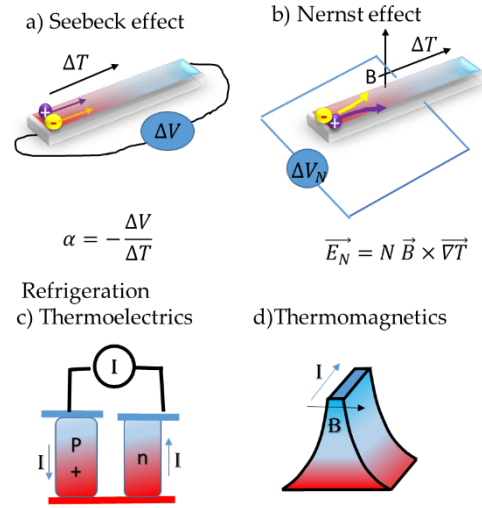
In non-degenerate semiconductors, the Seebeck coefficient increases as the bandgap increases. Within the single-band model, the further the chemical potential from the band edge, the larger the Seebeck coefficient. Within the two-band model that includes the conduction band and the valence band, the Seebeck coefficient increases with the ratio of the effective masses of the two bands and is zero close to the middle of the bandgap. Understanding how the Seebeck coefficient depends on the materials parameters helps in the design of highly efficient thermoelectric materials. [23–25] Perhaps, a better criterion is the thermoelectric power factor, but the Seebeck coefficient comes as the first step.

Similarly, the Nernst theory has also been studied in the past. Sondheimer studied the galvanometric and thermomagnetic effects in metals with s and d bands [17,26]. Putley [15] studied the Nernst signal in semiconductors through the Lorentz-Sommerfeld theory [27]. He started from a formalism developed by Sommerfeld and Frank [28] for metals and extended it to semiconductors and mixed conductors. [29] Theoretical predictions of the Nernst coefficient of PbTe and PbSe appeared to be reasonably close to experimental values. Price [30] obtained a relatively simple formula for the Nernst coefficient in the case of isotropic two-band semiconductors using Boltzmann statistics. In terms of electrical conductivity (σ), and Hall mobility (μ_H) of each band, the Nernst coefficient was defined as $N = k_B/e \left[\left(\frac{\sigma_e \sigma_h}{\sigma^2} \right) (\mu_e^H + \mu_h^H)(\alpha_e + \alpha_h) + \frac{\sigma_e \varphi_e + \sigma_h \varphi_h}{\sigma} \right] B$ where $\alpha_i = \frac{Td(\log n_i)}{dT} + \gamma_i$ and $\varphi_i = \gamma_i (\lambda_i^H - \mu_i^H)$. Based on the kinetic theory represented by Einstein [31], γ parameter relates diffusion coefficient to mobility by $\gamma_i = \frac{eD_i^T}{\mu_i k_B}$ and λ^H is a mobility developed by both magnetic field and temperature gradient. Jeffrey Clayhold studied the Nernst effect in anisotropic materials and found that the value of the Nernst coefficient depends on the correlation between the Hall angle and thermopower at different points on the Fermi surface [6]. Masuki et. al., using a momentum-dependent relaxation time approximation, showed that in $FeSb_2$, a second peak appears in the temperature dependence of the Nernst coefficient due to the phonon-drag effect [32]. Pikulin et. al. compared the value of the Nernst coefficient in cuprate superconductors calculated using constant relaxation time approximation (CRTA) and momentum-dependent relaxation time approximation [33]. They found that in the combined presence of the band and scattering anisotropy, the CRTA is a poor approximation and can result in an error significant enough to result in a Nernst coefficient of the wrong sign. It is noteworthy to mention here that, in their calculation, only the single band elastic quasi-particle scattering was considered, and the response in the low magnetic field limit was computed. In recent years, there has been a surge in

research activity concentrated on the Nernst effect in Weyl and Dirac semimetals. Consequently, several theoretical studies focusing on both the conventional and the anomalous part of the Nernst coefficient have been performed using the Boltzmann transport equation (BTE) [34,35]. The contribution of Berry curvature [35–38], conformal anomaly [39], gravitational and thermal chiral anomaly [40] in the anomalous part of the Nernst coefficient in these material systems have also recently been theoretically investigated. These works focus on the topological aspects of the problem but use approximations such as Mott's formula, Sommerfeld expansion, and small magnetic fields.

The goal of this paper is to find explicit and general analytical expressions for the Nernst coefficient in simple semiconductors and to develop an understanding of when large Nernst coefficient values are expected theoretically, hence narrowing down the search for good thermomagnetic materials. We use the term simple semiconductors in contrast to topological and ferromagnetic materials which are often used in the study of the Nernst coefficient. When possible and needed, we study the thermomagnetic power factor and lay the criteria for thermomagnetic transport. While similar results are available in old literature, there are several problems. First, they are scattered in old papers. Second, they are obtained sometimes using phenomenological assumptions and sometimes with little details of the assumptions used, and third, different authors obtained different equations using different assumptions. Here we use a BTE approach within the relaxation time approximation to study the Nernst coefficient under different band structures and scattering rates. When possible, we compare our results with previously obtained equations for the Nernst coefficient in simple semiconductors.

3. Analytical solutions:

3.1. General definition of the response functions:

First, we obtain the general solutions for the Nernst coefficient following Lundstrom's [41] and Smith's [42] notations. We start by expressing the electrical current (J) in terms of the electric field (E) and the gradient of the inverse temperature ($\nabla \left(\frac{1}{T} \right)$).

$$\boldsymbol{J} = \sigma \boldsymbol{E} + \beta \boldsymbol{\nabla} \left(\frac{1}{T} \right) \qquad\qquad 1$$

where σ and β are 3×3 response function tensors representing respectively the electrical conductivity and thermoelectric function. In the presence of an external magnetic field (B), moving electrons experience an additional force $\boldsymbol{F} = -e\boldsymbol{E} - e\boldsymbol{v} \times \boldsymbol{B}$. As

a result, the response functions are modified, i.e., they become a function of the magnetic field ($\sigma(B)$ and $\beta(B)$).

We start by first expressing the Nernst coefficient in terms of these matrices. The isothermal Nernst coefficient is defined as the ratio of the transverse voltage to an applied thermal gradient when the applied magnetic field is perpendicular to the directions of measured voltage and temperature gradient: $N_T = E_y/\nabla_x T$. This is subject to open-circuit electrical boundary conditions, *i.e.*, $J = 0$.

Denoting the resistivity tensor by $\rho = \sigma^{-1}$, we have $E = \rho\beta\nabla T/T^2$. In the presence of a magnetic field, we define the generalized Seebeck tensor as:

$$\alpha = \frac{\rho\beta}{T^2} \qquad\qquad 2$$

 In the case where the temperature gradient is along x, and the applied magnetic field along z, the longitudinal xx component in the B=0 limit is the ordinary Seebeck coefficient, while the transverse xy component contains the Nernst coefficient. We will show the explicit formula for $N_T = \alpha_{xy}$ in the next section.

3.2. General Solution of the BTE in the presence of a magnetic field within the relaxation time approximation:

If we denote the equilibrium distribution function by f^0, for every electronic state of momentum, k, and band index, n, the BTE is:

$$\frac{\partial f_{kn}}{\partial t} + v_{kn}.\nabla_r f_{kn} - e(E + v_{kn} \times B).\nabla_k f_{kn} = -\frac{f_{kn}-f_{kn}^0}{\tau_{kn}} \qquad\qquad 3$$

From now on, for simplicity, we omit the indices k,n from the velocities, electron energies, and distribution functions. Following Smith et al. [42] we write the solution to this equation in the form:

$$f = f^0 + \tau v.S\left(-\frac{\partial f^0}{\partial \varepsilon}\right) \qquad\qquad 4$$

where ε is the electron energy and the unknown vector S is assumed to be only a function of energy ε. Plugging this expression into BTE (3) yields the equation satisfied by S. It is well-known that in the absence of a magnetic field, S is the driving electrothermal force

F on the electrons: $S = F = -\nabla\varepsilon_f - \frac{\varepsilon-\varepsilon_f}{T}\nabla T$, where ε_f is the electrochemical potential (we are using μ to denote mobility). In the presence of **B**, and in steady-state, the BTE simplifies to:

$$(1 + \tau\Omega)f_1 = \tau\boldsymbol{v}.\boldsymbol{F}\left(-\frac{\partial f^0}{\partial\varepsilon}\right) \qquad\qquad 5$$

where we defined $\Omega = \frac{-e}{\hbar}(\boldsymbol{v}\times\boldsymbol{B}).\boldsymbol{\nabla}_k$ and $f_1 = f - f^0$. The operator Ω and namely $\boldsymbol{\nabla}_k$ acts on f_1 which is postulated to be of the form: $\tau\boldsymbol{v}.\boldsymbol{S}\left(-\frac{\partial f^0}{\partial\varepsilon}\right)$

This expression can be simplified if we assume the relaxation times depend only on the energy so that $\boldsymbol{\nabla}_k\tau = \frac{\partial\varepsilon}{\partial\boldsymbol{k}}\frac{\partial\tau}{\partial\varepsilon} = \hbar\boldsymbol{v}\frac{\partial\tau}{\partial\varepsilon}$. Furthermore, its action on the velocity gives the effective mass tensor at the point k: $\boldsymbol{\nabla}_k\boldsymbol{v} = \hbar\frac{1}{M}$ where M is the effective mass tensor. Inserting these relations into Eq. 5, one finds that $\boldsymbol{S}$ must satisfy.

$$\boldsymbol{S} - \omega\tau\,\widehat{\boldsymbol{B}}\times\mathbb{N}\,\boldsymbol{S} = \boldsymbol{F} \qquad\qquad 6$$

Where $\widehat{B}$ is the unit vector along the direction of the magnetic field, $\omega = \frac{eB}{m_0}$ is the cyclotron frequency, and the dimensionless 3×3 tensor $\mathbb{N}$ is the inverse effective mass matrix normalized by the bare electron mass m_0. Note that one can substitute the cross product by the multiplication by an antisymmetric matrix which we call $\mathfrak{B}$:

$$\mathfrak{B} = -\omega\tau\begin{pmatrix} 0 & -\widehat{B}_z & \widehat{B}_y \\ \widehat{B}_z & 0 & -\widehat{B}_x \\ -\widehat{B}_y & \widehat{B}_x & 0 \end{pmatrix} \qquad\qquad 7$$

So that the equation satisfied by **S** becomes a simple 3×3 linear system easily invertible.

$$\boldsymbol{S} = \mathbb{Q}\,\boldsymbol{F} \text{ with } \mathbb{Q} = (\mathbb{I} + \mathfrak{B}\mathbb{N})^{-1} \qquad\qquad 8$$

Therefore, in an actual calculation, if the band structure is known at any k-point of interest, one needs to calculate the group velocity and inverse effective mass tensor at that k-point, and use the solution to Eq. 8 to deduce the components of **S**, which will give the electrical current as:

$$\boldsymbol{J} = \frac{-e}{V}\sum_{kn}\boldsymbol{v}_{kn}\otimes\boldsymbol{v}_{kn}.\boldsymbol{S}_{kn}\,\tau_{kn}\left(-\frac{\partial f_{kn}^0}{\partial\varepsilon}\right) \qquad\qquad 9$$

This general solution has the advantage that is valid for any arbitrary orientation of the fields with respect to each other (no need to be perpendicular) or to the crystalline axes, is valid even at moderately large magnetic fields (within the semiclassical approximation) as long as we have a relaxation time that is only energy-dependent. If that is not the case, as an approximation, one may take its angular average over the constant energy surfaces of interest: $\tau_n(\varepsilon) = \sum_k \tau_{nk}\, \delta(\varepsilon - \varepsilon_{nk})$

Before proceeding further, we need to point out that although the Nernst coefficient is linear in B at small magnetic fields, the solution obtained above has in principle full magnetic field dependence as the distribution function has not been Taylor expanded in powers of B as is commonly done. In this limit, since we have $S + \mathfrak{B}\mathbb{N}\, S = F$, the solution becomes $S = (1 + \mathfrak{B}\mathbb{N})^{-1} F \approx F - \mathfrak{B}\mathbb{N}\, F$, i.e. we obtain the standard distribution function plus a correction linear in B: $\mathfrak{B}\mathbb{N} = eB\tau/m^*$ usually denoted by $\omega\tau$.

Behavior at high magnetic fields: From the above equation defining S, we can note that the behavior of response functions will then start with a constant plus a term linear in B at low B, and decays as $1/B$ at large fields. The crossover point is when $\omega\tau = \mu B \simeq 1$ where $\mu = e\,\langle \tau/m^* \rangle$ is the mobility of the sample. The behavior at these intermediate fields may be less straightforward in complex materials with large anisotropies in effective mass and relaxation time, but the limiting behavior will remain linear in B at low B and linear in $1/B$ at high B. At yet higher fields such that the cyclotron radius defined by $l_c^2 = \hbar/qB$ becomes smaller than other length scales in the problem such as the electron mean free paths, quantization effects become important, and the semiclassical BTE approach ceases to be valid.

Throughout the rest of this article, we fix the direction of the applied thermal gradient to be in the x-direction and the external magnetic field to be in the z-direction, irrespective of the crystalline axes. The Nernst voltage is then collected along y.

We focus on the *isothermal* Nernst coefficient N_T, where it is assumed there is no thermal gradient along y or z.

Using Eqs. 8 and 9, we can obtain the transport functions. First, to simplify notations, we define un-normalized transport averages as:

$$\langle\langle A \rangle\rangle_{ij} = \frac{1}{V}\sum_{nk} A_{nk}\, v_{nk}^i\, v_{nk}^l\, \mathbb{Q}_{lj}(n)\left(-\frac{\partial f_{nk}^0}{\partial \varepsilon}\right) \qquad\qquad 10$$

where implicit summation over repeated Cartesian indices $(i, j, l, ...)$ is implied. From their definition in Eq. 1, the general equations defining the response functions can be written as:

$$\sigma_{ij} = q^2 \langle\langle \tau \rangle\rangle_{ij} \quad ; \beta_{ij} = qT \langle\langle \tau(\varepsilon - \varepsilon_f) \rangle\rangle_{ij} \tag{11}$$

The normalizing factor $\langle\langle 1 \rangle\rangle_{ii} = \frac{1}{V} \sum_{nk} v_{nk}^i v_{nk}^l \mathbb{Q}_{li}(n)(-\frac{\partial f_{nk}^0}{\partial \varepsilon})$ can be derived to be $\frac{n}{m^*}$ in the isotropic case where the effective mass tensor is a scalar (n is the so-called free-electron density).

The Nernst voltage is measured under open-circuit conditions implying $J_x = J_y = 0$. Setting these currents to zero, and solving for E_x and E_y in terms of $\nabla_x T$ by using Eqs. 1, in agreement with previous work [10], the Nernst and Seebeck coefficients become:

$$N_T = \frac{E_y}{\nabla_x T} = \frac{1}{T^2} \frac{\sigma_{xx}\beta_{yx} - \sigma_{yx}\beta_{xx}}{\sigma_{xx}\sigma_{yy} - \sigma_{yx}\sigma_{xy}} \quad ; \quad \alpha_{xx} = \frac{E_x}{\nabla_x T} = \frac{1}{T^2} \frac{\sigma_{yy}\beta_{xx} - \sigma_{yx}\beta_{xy}}{\sigma_{xx}\sigma_{yy} - \sigma_{yx}\sigma_{xy}} \tag{12}$$

Equation 12 is valid for any arbitrary band structure as long as the x, y, z directions are defined along $\nabla T, \Delta V, B$ directions respectively.

3.3. Weak magnetic field limit:

In this section, we proceed to solve the problem in special cases where it can be solved analytically. Starting from Eqs. 12 and the following definitions, we need to find explicit solutions for $\sigma(B)$ and $\beta(B)$.

In the case of weak magnetic fields, Eq. 5 simplifies to $f_1 \approx (1 - \tau\Omega)\tau \boldsymbol{v}.\boldsymbol{F}\left(-\frac{\partial f^0}{\partial \varepsilon}\right)$. The first term is independent of the magnetic field and we express it as $f' = \tau \boldsymbol{v}.\boldsymbol{F}\left(-\frac{\partial f^0}{\partial \varepsilon}\right)$ and the second term is linear to $\boldsymbol{B}$ and we can express it as $f'' = \tau^2 \frac{e}{\hbar}(\boldsymbol{v} \times \boldsymbol{B}).\nabla_k(\boldsymbol{v}.\boldsymbol{F})\left(-\frac{\partial f^0}{\partial \varepsilon}\right)$. In writing f'', we assumed τ depends only on energy. The current is then written as $\boldsymbol{J} = \frac{-e}{V}\sum_k \boldsymbol{v} f_1$. Using the notation of Eq. 1 and after inserting f_1 into the current equation, we obtain: [41].

$$\sigma_{ij} = \frac{e^2}{V}\sum_k \tau\left(-\frac{\partial f^0}{\partial \varepsilon}\right) v_i(v_j + \frac{e}{\hbar}\tau \in_{mnp} v_m B_n \frac{\partial v_j}{\partial k_p}) \tag{13}$$

$$\beta_{ij} = -\frac{ek_B T^2}{V}\sum_k \tau\left(-\frac{\partial f^0}{\partial \varepsilon}\right) v_i(x - x_f)(v_j + \frac{e}{\hbar}\tau \in_{mnp} v_m B_n \frac{\partial v_j}{\partial k_p}) \tag{14}$$

Implicit summation over repeated indices is implied. k_B is the Boltzmann constant, $\in_{mnp}$ is the antisymmetric Levi-Civita symbol, and x refers to dimensionless (reduced) energy $x = \frac{\varepsilon}{k_B T}$ throughout this work.

3.4. Special cases

3.4.1. Case of isotropic single band:
A single band with isotropic effective mass is the simplest possible band structure and hence that will be our starting point. In this case, the derivative of the velocity with respect to momentum is the inverse of the effective mass ($\frac{\partial v_j}{\partial k_i} = \hbar \frac{\delta_{ji}}{m^*}$). Considering the magnetic field is in the z-direction, Eq. 13 for the isotropic case simplifies to:

$$\sigma_{ij} = \frac{e^2}{V}\sum_k \tau \left(-\frac{\partial f^0}{\partial \varepsilon}\right) v_i v_j + \frac{1}{V}\sum_k \frac{e^3\tau^2}{m^*}\left(-\frac{\partial f^0}{\partial \varepsilon}\right) \in_{mzj} v_i v_m B_z \qquad 15$$

If we now define normalized transport averages by: $\langle A \rangle_{ij} = \sum_k A_k\, v_i v_j \left(-\frac{\partial f^0}{\partial \varepsilon}\right)/ \sum_k v_i v_j \left(-\frac{\partial f^0}{\partial \varepsilon}\right)$ we have:

$$\sigma_{xx} = \sigma_{yy} = \frac{e^2}{V}\sum_k \tau \left(-\frac{\partial f^0}{\partial \varepsilon}\right) v_x v_x = \frac{e^2}{V}\frac{N}{m^*}\langle \tau \rangle = \sigma_0 \qquad 16$$

$$\sigma_{xy} = -\sigma_{yx} = -\frac{1}{V}\sum_k \frac{e^3\tau^2}{m^*}\left(-\frac{\partial f^0}{\partial \varepsilon}\right) v_x v_x B_z = -\mu_H \sigma_0 B_z \qquad 17$$

where $N = \sum_k m^* v_i v_j \left(-\frac{\partial f^0}{\partial \varepsilon}\right)$ is the number of free carriers, and $\mu_H = \frac{e}{m^*}\frac{\langle \tau^2 \rangle}{\langle \tau \rangle}$ is the Hall mobility. Since we are dealing with isotropic band structure, we drop the xx index from the averaging.

Similarly, Eq.14 under isotropic conditions is:

$$\beta_{xx} = \beta_{yy} = -\frac{ek_BT^2}{V}\sum_k \tau \left(-\frac{\partial f^0}{\partial \varepsilon}\right) v_x v_x (x - x_f) = -\frac{eT}{V}\langle \tau(\varepsilon - \varepsilon_f)\rangle \frac{N}{m^*} = \beta_0 \qquad 18$$

$$\beta_{xy} = -\beta_{yx} = \frac{k_BT^2}{V}\sum_k \frac{e^2\tau^2}{\hbar m^*}\left(-\frac{\partial f^0}{\partial \varepsilon}\right) v_x v_x B_z (x - x_f) = -\beta_0 \mu_\beta B_z \qquad 19$$

where $\mu_\beta = \frac{e}{m^*}\frac{\langle \tau^2 (\varepsilon - \varepsilon_f)\rangle}{\langle \tau (\varepsilon - \varepsilon_f)\rangle}$ and we refer to it as thermal mobility.

By substituting all transport functions obtained above in Eq. 12 we find:

$$N_T = \alpha_0 \frac{(\mu_\beta - \mu_H)}{(1 + (\mu_H B_z)^2)} B_z \quad \text{where the zero-field Seebeck is } \alpha_0 = \beta_0/T^2\sigma_0 \qquad 20$$

This is our first significant result stating that the Nernst coefficient is proportional to the Seebeck coefficient (α_0) and also to the difference between the thermal and Hall mobilities. We notice that under constant relaxation time approximation, μ_β and μ_H are identical and the Nernst coefficient is zero! Hence, in the isotropic single band model, the Nernst coefficient is merely the result of energy-dependent scattering rates.

We can further include power laws for the relaxation times to better understand the relation between the Nernst coefficient and the energy dependence of the relaxation times. It is shown that the relaxation times can be approximated by power laws in the form of $\tau = \tau_0 x^s$ for several common scattering mechanisms. For instance the scattering parameter (or characteristic exponents), s, is -0.5 for acoustic phonon scattering and 1.5 for weakly screened ionized impurity scattering. [41] In general since only electrons in a narrow Fermi window contribute to transport, it is possible to fit the scattering rates with a power law form. Assuming a power law for scattering rates, we obtain:

$$\mu_H = \frac{e}{m^*}\frac{<\tau^2>}{<\tau>} = \mu_0 \frac{(2s+1.5)}{(s+1.5)}\frac{F_{2s+0.5}(x_f)\Gamma(2s+1.5)}{F_{s+0.5}(x_f)\Gamma(s+1.5)} \qquad 21$$

$$\mu_\beta = \mu_0 \frac{(2s+2.5)(2s+1.5)F_{2s+1.5}(x_f)-x_f(2s+1.5)F_{2s+0.5}(x_f)}{(s+2.5)(s+1.5)F_{s+1.5}(x_f)-x_f(s+1.5)F_{s+0.5}(x_f)}\frac{\Gamma(2s+1.5)}{\Gamma(s+1.5)} \qquad 22$$

Here, s is the scattering parameter, $\mu_0 = \frac{e\tau_0}{m^*}$ is the constant mobility, and $x_f = \frac{\varepsilon_f}{k_B T}$ is the reduced chemical potential. As can be seen, it is possible to obtain analytical solutions in the general case, but not simple to interpret as they include Fermi Dirac integrals ($F_j(x_f)$) and gamma functions (Γ). Figure 2 shows the plot of these solutions for the Nernst coefficient as a function of the modified chemical potential for several s-values. We note that solutions do not exist for all possible s-values. The Nernst coefficient increases as the s-parameter increases. We can conclude that the Nernst coefficient is larger when there is a stronger energy dependence of the differential conductivity.
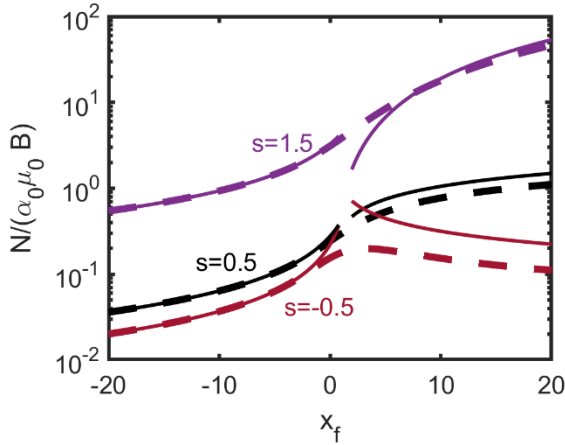

Figure 2. The ratio of the Nernst to Seebeck coefficient as a function of the reduced chemical potential ($x_f = \frac{\varepsilon_f}{k_B T}$). Zero is the band edge. Dashed lines are the general solutions of the isotropic bands, Eq. 20, obtained by subtracting Eq. 21 from 22 (the two mobilities). Solid lines at the negative side are showing the non-degenerate solutions of Eq. 24. As expected only at negative Fermi levels, non-degenerate solutions match the full solutions. Solid lines at positive Fermi levels are degenerate approximations using the Sommerfeld expansion Eq. 27. Note that the absolute values are plotted, and the second order B terms $(\mu_H B_z)^2$ are ignored.

Nondegenerate case: Using non-degenerate (Maxwell-Boltzmann) statistics, it is possible to further simplify the equations. Doing so, we obtain

$$\mu_\beta - \mu_H = \mu_0 \left(\frac{s}{s+2.5-x_f}\right)\frac{\Gamma(2s+2.5)}{\Gamma(s+2.5)} \qquad 23$$

$$N_T = \frac{\alpha_0}{(1+(\mu_H B_z)^2)}\left(\frac{s}{s+2.5-x_f}\right)\frac{\Gamma(2s+2.5)}{\Gamma(s+2.5)}\mu_0 B_z \qquad 24$$

The results of Eq. 24 are only valid in the non-degenerate limit when the chemical potential is in the gap (negative). The analytical solutions of Eq. 24 are plotted in Figure 2 (solid lines in the negative x_f range. They can closely reproduce the full solutions represented in Eqs. 20, 21, and 22 (dashed lines). In the nondegenerate case, the $\frac{N}{\alpha_0}$ ratio decreases as the chemical potential moves away from the band-edge (as $\frac{1}{s+2.5-x_f}$). However, we note that the α_0 increases linearly as the chemical potential moves away from the band edge as $(x_f - s - 2.5)$. Hence, N does not have any significant chemical potential dependence! The results obtained in Eq. 24 are similar to what Delves [10] presented in his comprehensive review for spherical bands and non-degenerate statistics (see Eq. 5.10 of Ref. 10). The difference is the extra factor of $\frac{\Gamma(2s+2.5)}{\Gamma(s+2.5)}$ in our results. Delves obtained his results by modifying the distribution function by a $\frac{1}{(1+(\omega\tau)^2)}$ factor in the presence of an external magnetic field where $(\omega = \frac{eB}{m^*})$ is the cyclotron resonance frequency.

Degenerate case: We can also estimate the solutions in the metallic (degenerate case). To find μ_H, we approximate $\frac{\partial f^0}{\partial \varepsilon} \sim \delta(\varepsilon - \varepsilon_f)$ and we obtain:

$$\mu_H = \frac{e}{m*} \frac{\int \tau^2 \delta(\varepsilon-\varepsilon_f) v_x v_x g(\varepsilon) d\varepsilon}{\int \tau \delta(\varepsilon-\varepsilon_f) v_x v_x g(\varepsilon) d\varepsilon} = \mu_0\, x_f^s \qquad\qquad 25$$

The same approximation for μ_β gives zero due to the $(\varepsilon - \varepsilon_f)$ term and hence, we use the Sommerfeld expansion to obtain:

$$\mu_\beta = \mu_0 \frac{\int x^{2s}\left(\frac{\partial f^0}{\partial \varepsilon}\right) v_x v_x g(\varepsilon)(\varepsilon-\varepsilon_f) d\varepsilon}{\int x^s\left(\frac{\partial f^0}{\partial \varepsilon}\right) v_x v_x g(\varepsilon)(\varepsilon-\varepsilon_f) d\varepsilon} = \mu_0 \frac{2(2s+1.5)x_f^{2s+0.5}}{2(s+1.5)x_f^{s+0.5}} = \mu_0 x_f^s \frac{(2s+1.5)}{(s+1.5)} \qquad 26$$

Plugging Eqs. 25 and 26 into 20 we obtain:

$$N_T = \frac{\alpha_0}{(1+(\mu_H B_z)^2)} x_f^s \frac{s}{(s+1.5)} \mu_0 B_z \qquad\qquad 27$$

The results of Eq. 27 are only valid in the degenerate (metallic) case when the chemical potential is well-inside the band (positive). These results are also plotted in Figure 2 (solid lines on the positive x_f side) and can reproduce full solutions especially when s is larger than 1. In Eq. 27, when s is positive, $\frac{N_T}{\alpha_0}$ increases with the chemical potential. When s is

negative, the ratio decreases with increasing the chemical potential. We also remind the reader that α_0 itself has $\frac{1}{x_f}$ dependence. Hence in this limit, N is proportional to x_f^{s-1}.

Within the same approximations used to obtain Eq. 27, the Seebeck coefficient can be expressed as $\left(\alpha_0 = \frac{\pi^2}{3}\frac{k_B}{e}\frac{(s+1.5)}{x_f}\right)$ and hence the Nernst coefficient is $N_T = \frac{\pi^2}{3}\frac{k_B}{e}\frac{s\,x_f^{s-1}}{(1+(\mu_H B_z)^2)}\mu_0 B_z$, ignoring the second-order B term. This is similar to (but not identical to) $N_T = \frac{\pi^2}{6}\frac{k_B}{e}\frac{1}{x_f}\mu_0 B_z$ obtained by Feiber et.al. [43,44]. They used nearly free-electron picture with a phenomenological relaxation time approximation and assumed the Fermi level is much larger than the thermal energy (strong metal) to obtain their expression. Moreau [45] has developed a phenomenological relation for the Nernst coefficient in metals $\left(N_T = R_H \sigma \left(T\frac{d\alpha_0}{dT}\right)B\right)$. It seems that Moreau argument has been an analogy to the Hall effect which he attributed to some sort of deformation. While he has not provided a convincing proof, he has shown that his relation can explain some of the experimental observations in metals. [46] It has shown that his relation can also explain some of the semiconductor trend. [14,47] We notice that within single band degenerate model, α_0 is linear in T and hence $T\frac{d\alpha_0}{dT} = \alpha_0$ and $R_H \sigma = \mu_H = \mu_0 x_f^s$. Hence, Moureau's relation is similar to what we obtained here in Eq. 27. Ignoring the second-order B term, the difference is a factor of $\frac{s}{(s+1.5)}$.

3.4.2. Case of ellipsoidal single-band: The analysis of the isotropic case points to the fact that anisotropy can increase the Nernst coefficient. Hence, here we study the case where the effective mass is different along different axes and the dispersion relation is $\varepsilon = \frac{\hbar^2}{2}\left(\frac{k_x^2}{m_x} + \frac{k_y^2}{m_y} + \frac{k_z^2}{m_z}\right)$. Using the same steps as before and observing that $\frac{dv_i}{dp_j} = \frac{\delta_{ij}}{m_i}$, we can start from Eq. 13 to obtain:

$$\sigma_{xx} = \frac{e^2}{V}\sum_p \tau\left(-\frac{\partial f^0}{\partial \varepsilon}\right)v_x v_x \tag{28}$$

$$\sigma_{xy} = -\frac{1}{V}\sum_p \frac{e^3\tau^2}{m_y^*}\left(-\frac{\partial f^0}{\partial \varepsilon}\right)v_x v_x B_z = -\mu_{Hxy}\sigma_{xx}B_z \tag{29}$$

$$\mu_{Hxy} = \frac{e}{m_y^*}\frac{\sum_p \tau^2\left(-\frac{\partial f^0}{\partial \varepsilon}\right)v_x v_x}{\sum_p \tau\left(-\frac{\partial f^0}{\partial \varepsilon}\right)v_x v_x} = \frac{e}{m_y^*}\frac{<\tau^2>_{xx}}{<\tau>_{xx}} \tag{30}$$

In defining mobility, the first index refers to the direction of velocities over which the averaging is performed, and the second index refers to the effective mass direction.

$$\sigma(B) = \begin{bmatrix} \sigma_{xx} & -\sigma_{xx}\mu_{Hxy}B \\ \mu_{Hyx}\sigma_{yy}B & \sigma_{yy} \end{bmatrix} \tag{31}$$

The transport matrices are 3×3 but since we fixed B in the z-direction, to keep things simple, we only use 2×2 matrices. Similarly

$$\beta(B) = \begin{bmatrix} \beta_{xx} & -\beta_{xx}\mu_{\beta_{xy}}B \\ \mu_{\beta_{yx}}\beta_{yy}B & \beta_{yy} \end{bmatrix} \qquad\qquad 32$$

$$\mu_{\beta_{xy}} = \frac{q}{m_y^*} \frac{<\tau^2\,(\varepsilon-\varepsilon_f)>_{xx}}{<\tau\,(\varepsilon-\varepsilon_f)>_{xx}} \qquad\qquad 33$$

The Seebeck tensor is then

$$\alpha(B) = \frac{\rho\beta}{T^2} = \frac{1}{\left(1+\mu_{H_{xy}}\,\mu_{H_{yx}}B^2\right)} \begin{bmatrix} \alpha_{xx} + \mu_{H_{xy}}\,\mu_{\beta_{yx}}\alpha_{yy}B^2 & -\alpha_{xx}\mu_{\beta_{xy}}B + \alpha_{yy}\mu_{H_{xy}}B \\ -\alpha_{xx}\mu_{H_{yx}}B + \mu_{\beta_{yx}}\alpha_{yy}B & \alpha_{yy} + \mu_{H_{yx}}\alpha_{xx}\,\mu_{\beta_{xy}}B^2 \end{bmatrix} \qquad 34$$

And the Nernst coefficient is the xy component of the Seebeck tensor.

$$N_T = \alpha_{xy}(B) = \frac{\left(\alpha_{yy}\,\mu_{H_{xy}} - \alpha_{xx}\,\mu_{\beta_{xy}}\right)B}{\left(1+\mu_{H_{xy}}\,\mu_{H_{yx}}\,B^2\right)} \qquad\qquad 35$$

Within the constant relaxation time, this equation simplifies to

$$N_T = \frac{\alpha_y - \alpha_x}{\left(1+\mu_{H_{xy}}\,\mu_{H_{yx}}\,B^2\right)}\,\mu_{0_{yy}}B_z \qquad\qquad 36$$

Here $\mu_{0_{yy}} = \frac{e\tau_0}{m_y^*}$ is the mobility in the y-direction. Eq. 36 shows that the Nernst coefficient is proportional to the difference between the Seebeck coefficients in the x and y directions. The more anisotropic a sample is, the higher the Nernst coefficient. For instance, in layered materials and superlattices, the in-plane transport coefficients are very different compared to the cross-plane transport coefficients. Hence these are good candidates to explore large Nernst coefficients. An extreme case would be if there is p-type transport in the x-direction and n-type transport in the y-direction. While unusual, materials with different polarity transport in in-plane and cross-plane directions have been observed and studied in the past. [48–53] It would be interesting to measure the Nernst coefficient of these materials.

Similar to the isotropic case, one can include energy-dependent relaxation times in a power-law form. Upon doing so we obtain:

$$N_T = \frac{\mu_{0yy}B}{\left(1+\mu_{H_{xy}}\mu_{H_{yx}}B^2\right)}\left(\alpha_{yy} - \alpha_{xx}\frac{2s+2.5-x_f}{s+2.5-x_f}\right)\frac{\Gamma(2s+2.5)}{\Gamma(s+2.5)}$$ 37 (non-degenerate)

$$N_T = \frac{\left(\alpha_{yy}-\alpha_{xx}\frac{(2s+1.5)}{(s+1.5)}\right)}{\left(1+\mu_{H_{xy}}\mu_{H_{yx}}B^2\right)}\,x_f^s\mu_{0yy}B$$ 38 (degenerate)
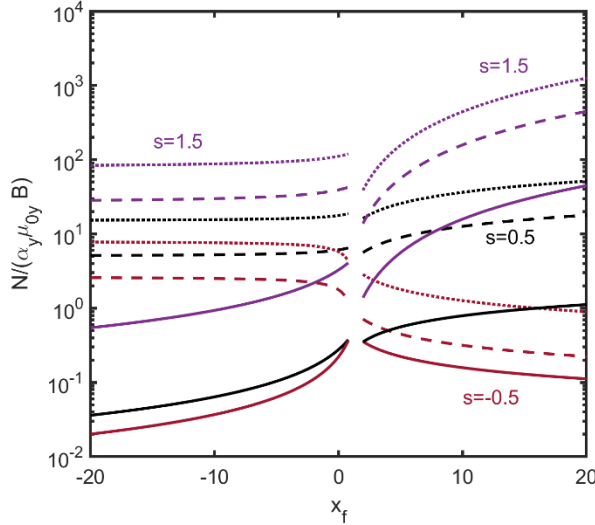

Figure 3. Ellipsoidal case: The absolute value of the Nernst coefficient divided by the y component of the Seebeck coefficient versus reduced chemical potential ($x_f = \frac{\varepsilon_f}{k_B T}$). The curves are plotted after Eq. 37 and 38 in the non-degenerate and degenerate limits, respectively. Solid lines are referring to when ($\frac{\alpha_y}{\alpha_x} = 1$) which is then like the isotropic case. Dashed lines are referring to when (($\frac{\alpha_y}{\alpha_x} = 4$) and dotted lines are plotted for ($\frac{\alpha_y}{\alpha_x} = 10$). Red, black, and purple refer to s parameters of -0.5, 0.5, and 1.5, respectively. Second order terms in B are ignored.

As seen in Eq. 37 (non-degenerate)37, 38, and Figure 3, the larger the ratio of the Seebeck coefficients in the two directions, the larger the Nernst coefficient. As before the Nernst coefficient is also an increasing function of the s-parameter.

3.4.3. The two-band model: The case of two bands is important since it allows investigation of the effect of bandgap and mass mismatch between electrons and holes. To keep the equations simple, here we assume that there are two isotropic bands, one is the conduction band labeled by e for electrons hereafter, and the other is the valence band labeled by h for holes. We start from Eq. 12 and define each component in the presence of two bands. Since the current of electrons and holes are additive, we find that

$$\sigma_{ij} = \sigma_{ij}^e + \sigma_{ij}^h$$ 39

$$\beta_{ij} = \beta^e_{\ ij} + \beta_{ij}^h$$ 40

We note that the conductivity term that does not have B dependence has the same sign for electrons and holes, while the conduction term that is linear in B has opposite signs for electrons and holes. In the thermoelectric coefficients β however, the terms with no B-

field are linear in charge (and opposite in sign) and those linear in B are in e^2. We note that equations for single-band were developed for electrons assuming a charge of $-e$, hence some of the signs are modified for the case of holes. To be able to address the two bands properly, we revise our definitions with the isotropic conditions for each band in mind. Each band starts at ε_0 and goes to infinity. (That is the axis is flipped when dealing with the valence band)

Defining:

$$
\begin{cases}
\sigma_0 = \int_{\varepsilon_0}^{\infty} e^2 \tau \left(-\frac{\partial f^0}{\partial \varepsilon}\right) v_x v_x \, g(\varepsilon - \varepsilon_0) d\varepsilon \\
\beta_0 = \int_{\varepsilon_0}^{\infty} e\tau T \left(-\frac{\partial f^0}{\partial \varepsilon}\right) v_x v_x \left(\varepsilon - \varepsilon_f\right) g(\varepsilon - \varepsilon_0) d\varepsilon \\
\mu_H = \frac{e}{m^*} \frac{<\tau^2>}{<\tau>} \\
\mu_\beta = \frac{e}{m^*} \frac{<\tau^2(\varepsilon - \varepsilon_f)>}{<\tau(\varepsilon - \varepsilon_f)>}
\end{cases}
\qquad 41
$$

And using superscripts e/h for electrons and holes we obtain

$$
\begin{cases}
\sigma_{xx} = \sigma_0^e + \sigma_0^h \\
\sigma_{xy} = \left(-\mu_H^e \sigma_0^e + \mu_H^h \sigma_0^h\right) B_z \\
\beta_{xx} = -\beta_0^e + \beta_0^h \\
\beta_{xy} = \left(\beta_0^e \mu_\beta^e + \beta_0^h \mu_\beta^h\right) B_z
\end{cases}
\qquad 42
$$

Plugging Eq. 42 into Eq. 12 and ignoring second-order B terms, we find:

$$
N_T = \frac{-1}{T^2} \frac{\left(\sigma_0^e + \sigma_0^h\right)\left(\beta_0^e \mu_\beta^e + \beta_0^h \mu_\beta^h\right) + \left(\mu_H^e \sigma_0^e - \mu_H^h \sigma_0^h\right)\left(-\beta_0^e + \beta_0^h\right)}{\left(\sigma_0^e + \sigma_0^h\right)^2} B_z
\qquad 43
$$

$$
N_T = \frac{\left(\sigma_0^{e^2} N_e + \sigma_0^{h^2} N_h\right)}{\left(\sigma_0^e + \sigma_0^h\right)^2} - \frac{1}{T^2} \frac{\sigma_0^e \beta_0^h \left(\mu_\beta^h + \mu_H^e\right) + \sigma_0^h \beta_0^e \left(\mu_\beta^e + \mu_H^h\right)}{\left(\sigma_0^e + \sigma_0^h\right)^2} B_z
\qquad 44
$$

Where $N_e = \frac{1}{T^2} \frac{\beta_0^e \left(\mu_\beta^e - \mu_H^e\right)}{\sigma_0^e} B_z$ is the Nernst coefficient of the conduction band alone and $N_h = \frac{1}{T^2} \frac{\beta_0^h \left(\mu_\beta^h - \mu_H^h\right)}{\sigma_0^h} B_z$ is the Nernst coefficient of the valence band alone.

The first term in the Nernst coefficient is a weighted average of the Nernst coefficients of the electrons and holes, weighted by conductivity squared. The second term is a mixed contribution of the two bands. We refer to the first term as the "*average Nernst*" and the second term as the "*mixed Nernst*" term.

To keep the calculations simple, we study Eq. 44 under constant relaxation time approximation (CRTA). In the isotropic single band model case, the Nernst coefficient was found to be zero under CRTA. The two mobilities $\mu_H = \mu_\beta = \frac{e\tau_0}{m^*}$ were identical, hence $N_e = N_h = 0$. In the two-band model, and under CRTA, the average Nernst term is therefore zero. However, the mixed Nernst term containing the cross terms between the two bands results in a nonzero Nernst coefficient (see Eq. 44).

Under CRTA, $\mu_H = \mu_\beta = \mu_0 = \frac{e\tau_0}{m^*}$. Defining $\alpha_0 = \frac{1}{T^2}\frac{\beta_0}{\sigma_0}$, Eq. 44 simplifies to:

$$N = -\frac{\sigma_0^e \sigma_0^h}{\left(\sigma_0^e + \sigma_0^h\right)^2}\left(\alpha_0^e + \alpha_0^h\right)\left(\mu_0^e + \mu_o^h\right) B_z \tag{45}$$

Observe that α_0 is similar to the Seebeck coefficient, but it has the contribution of only 1 band, and it is positive for both the conduction band and the valence band. A puzzling observation is that even when the two bands are identical and when we are at the center of the gap (full symmetry), the Nernst coefficient is not zero and it is equal to $N = -\alpha_0\mu_0 B_z$. While everything in our analysis of a single band model pointed to the requirement of asymmetry, here, we observe that the cross terms between the two bands result in a nonzero Nernst coefficient in the case of symmetrical bands.

We can further study Eq.45 assuming non-degenerate statistics (chemical potential in the gap). In the non-degenerate limit, we can define:

$$\begin{cases} \sigma_0^e = ne\mu_0^e; \sigma_0^h = pe\mu_0^h \\ n = N_c e^{-(x_c - x_f)}; p = N_v e^{-(x_f - x_v)} \\ \alpha_0^e = \frac{k_B}{e}\left(x_c - x_f + \frac{5}{2}\right); \alpha_0^h = \frac{k_B}{e}\left(x_f - x_v + \frac{5}{2}\right) \end{cases} \tag{46}$$

using these definitions, Eq .45 simplifies to:

$$N_T = -\frac{k_B}{e}\left(x_g + 5\right)\frac{\left(\mu_0^e + \mu_0^h\right)}{\left(n\mu_0^e + p\mu_0^h\right)^2} N_c N_v e^{-x_g}\mu_0^e\mu_0^h B_z \tag{47}$$

Figure 4 demonstrates the effect of bandgap and effective mass ratio on the Nernst coefficient. Here we plot the absolute value of Nernst divided by $\mu_0 B_z = \frac{e\tau_0}{m_0} B_z$ versus reduced chemical potential, we take the middle of the gap as zero and we assumed both electrons and holes have the relaxation time of τ_0. Hence the only relevant parameters are the reduced bandgap ($x_g = \frac{\varepsilon_g}{k_B T}$), the reduced chemical potential and the effective mass ratio ($m_r = \frac{m_h}{m_e}$), and the electronic mass (m_e, this is the mass relative to the free electron mass m_0, note that we could have divided everything by m_h instead and the results would be similar).

$$\left|\frac{N_T}{\mu_0 B_z}\right| = \frac{k_B}{e}\left(x_g + 5\right)e^{-x_g}\frac{(m_r + 1)m_r^{-0.5}}{m_e\left(e^{-\left(\frac{x_g}{2} - x_f\right)} + \sqrt{m_r}e^{-\left(x_f + \frac{x_g}{2}\right)}\right)^2} \tag{48}$$

In the middle of the gap, where the Seebeck coefficient is normally zero, the Nernst coefficient has its peak value. Similar to the Seebeck coefficient, the values of the Nernst coefficient increase as the bandgap increases. This is clear in Figure 4b where we fixed the mass ratio of electrons to holes to 1 ($m_e = m_h = 1$) and only modified x_g. We observe that the Nernst coefficient in this case linearly increases with the bandgap. Increasing the mass ratio of the electrons to holes (or vice versa) increases the Seebeck coefficient. However, this is not the case for the Nernst coefficient. Increasing the mass ratio lowers the Nernst coefficient as shown in Figure 4a. Finally, we notice that in Eq. *48*, there is a mass in the denominator. This means that the Nernst coefficient is larger for smaller effective mass values. Reducing the mass values to half increases the Nernst coefficient by a factor of 2.

Let us compare these results with that of Putley [15]. For mixed conductors, Putley obtained: $N_T = -\frac{3\pi k_B}{16e}\frac{(n^2\mu_e^3+p^2\mu_h^3)-np\mu_e\mu_h(\mu_h+\mu_e)(7+2x_g)}{(n\mu_e+p\mu_h)^2}B$ The first paranthesis in Putley is the individual contribution of conduction and valence band which is the equivalent of our average Nernst term. As discussed under CTRA this term is zero. Hence his expression reduces to $N_T = \frac{3\pi k_B}{16e}(7+2x_g)\frac{np\mu_e\mu_h(\mu_h+\mu_e)}{(n\mu_e+p\mu_h)^2}B$ which differs from our equation by a factor of $\frac{3\pi}{16}(7+2x_g)/(5+x_g)$. Putley's work is based on drift-diffusion model and assumes that the scattering is dominated by Debye longitudinal lattice model. We can also compare our results with what is presented by Aono [54] where he assumed the same scattering mechanism for electrons and holes. Similarly, keeping only mixed band contributions, Aono's expression can be written as $N_T = \frac{Ak_B}{e\sigma^2}(-\sigma_h\sigma_e)(\mu_h+\mu_e)(5+3s+x_g)B$. The A parameter is described by Aono as a positive numerical coefficient that is function of s. If we ignore this parameter and set s=0 (CRTA), then the results of Aono is similar to what we obtained in Eq. 47. However, we note that the start-point of both Aono and Putley seems to be degenerate conductors and the equations were then extended to mixed conductors. Finally, we compare the results to those of Price who obtained the Nernst coefficient for two isotropic bands using drift-diffusion model. The mixed term in Price's analysis (See Eq. 12' of Ref. [30]) is $N_T = \frac{k_B}{e}(x_g+3+\gamma_e+\gamma_h)\frac{(\mu_e+\mu_h)}{\sigma^2}\sigma_e\sigma_h B_z$ wherein γ_e and γ_h are unitless numbers connecting thermal diffusion coefficient and Einstein diffusion coefficients for electrons and holes. We see that the only difference between Eq. 47 and this one is the replacement of $(\gamma_e+\gamma_h)$ by 2, meaning our treatment is equivalent of ratio of 1 between the thermal and normal diffusion constants in Price analysis.

Beyond CTRA, it is easier to study the results numerically. What we obtained previously for isotropic single-bands and ellipsoidal bands remains valid. For instance, when

considering power law for relaxation times [$\tau = \tau_0 \left(\frac{\varepsilon}{k_B T}\right)^s$], the Nernst coefficient increases as the s-parameter increases. This is shown in Fig. 4c where we assumed identical bands (effective mass of 1 and the same s-parameter for the two bands) and $x_g = 10$. Results are plotted on the logarithmic axis and indicate enhancement in the Nernst coefficient as the s-parameter increases. Note that Fig. 4c is obtained numerically.
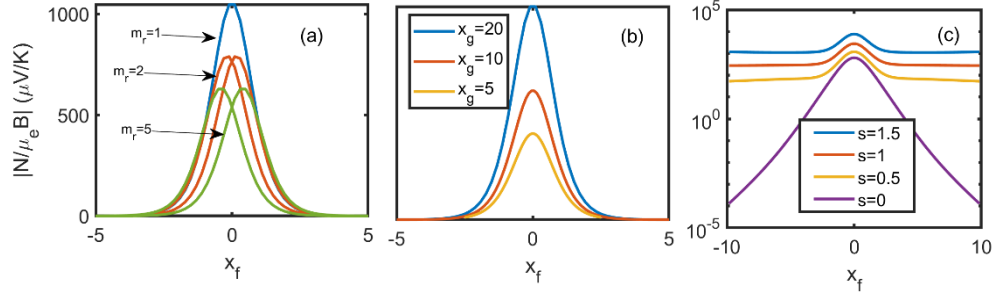

Figure 4. The absolute value of the Nernst coefficient divided by ($\mu_0 B = \frac{e\tau_0}{m_0} B$) is plotted versus reduced chemical potential (x_f) for the two-band model assuming isotropic bands under CRTA and assuming same τ_0 for both electrons and holes. Zero is the middle of the bandgap (a) The bandgap is $x_g = 20$, m_r is the ratio of effective mass of the two bands. If holes are heavier, the shift of the peak is toward the conduction band and vice-versa. e.g., m_r=2 is plotted once for m_e=1 and m_h=2 and again for m_h=1 and m_e=2 (b) The mass ratio is set to 1 and the bandgap is changed.

In analyzing the Nernst coefficient, we observed that the Nernst coefficient increases as the bandgap increases. This observation is against the general knowledge that the best thermomagnetic materials are semi-metals. To understand the benefit of the semimetals, it is not sufficient to study the Nernst coefficient, and we need to study the thermomagnetic power factor.

$$PF = \frac{\sigma}{\mu_0}\left|\frac{N_T}{\mu_0 B_z}\right|^2 = \frac{2k_B^2}{e}\left(\frac{2\pi kT}{h^2}\right)^{\frac{3}{2}}(x_g+5)^2\, e^{-2x_g}\,\frac{(m_r+1)^2}{m_r m_e^{1.5}\left(e^{-\left(\frac{x_g}{2}-x_f\right)}+\sqrt{m_r}e^{-\left(x_f+\frac{x_g}{2}\right)}\right)^3}$$

49

Figure 5 shows the behavior of the power factor. We observe that the power factor has a similar dependence on mass ratio as the Nernst coefficient. We also note that the power factor increases as the effective mass decreases. The optimum Power factor is when the mass ratio is 1. In this case, the optimum power factor is in the middle of the bandgap. Under these conditions, the thermomagnetic power factor can be simplified to

$$PF \propto \frac{(x_g+5)^2 e^{-\frac{x_g}{2}}}{m_e^{1.5}}$$

50

The power factor as a function of the reduced bandgap (x_g) is plotted in Figure 5b. We notice that the power factor decreases as the bandgap increases. This is

consistent with our understanding that narrow gap semiconductors and semimetals are good thermomagnetic candidates. Hence while the Nernst coefficient increases with bandgap, the thermomagnetic power factor decreases with bandgap.
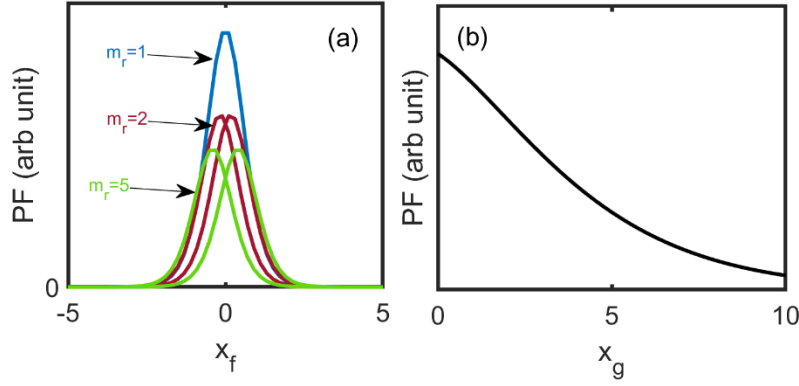

Figure 5. Power factor ($\sigma_{yy}N^2$) plotted after Eq. 52 using arbitrary unit. Parameters are similar to Fig.4 parameters. a) x_g=20 for all graphs; for $m_r = 1$:$m_e = m_h = 1$; for $m_r = 2$:$m_e = 1$ $m_h = 2$ and $m_e = 2$ $m_h = 1$; for $m_r = 5$:$m_e = 1$ $m_h = 5$ and $m_e = 5$ $m_h = 1$. b) $m_r = m_e = 1$, optimum PF (Eq.50) plotted vs reduced bandgap (x_g).

4. Conclusions:

In this work, we presented a description of the Nernst coefficient in simple conductors. Within an isotropic single band model, we obtained that the Nernst coefficient is zero in the CTRA. A nonzero Nernst coefficient in this case is the result of energy-dependent relaxation times and is proportional to the difference between thermal and Hall mobilities times the Seebeck coefficient. When using power laws and s-parameter to describe the relaxation times, we obtained that the Nernst coefficient is an increasing function of s. It is proportional to the Seebeck coefficient times mobility times magnetic field ($N \propto \alpha_0 \mu_0 B_z$). There is a factor of $\frac{1}{(1+(\mu_H B_z)^2)}$ which comes from the determinant of the conductivity tensor. In the nondegenerate limit, the Nernst coefficient does not have any explicit dependence on the chemical potential, and in the degenerate limit, it is proportional to x_f^{s-1}.

When the bands are anisotropic, the Nernst coefficient is nonzero even within the CTRA and it is proportional to the difference in the Seebeck coefficient of x and y directions. Hence, within one band model anisotropy in x-y crystallographic directions is

desired. Within the two-band model, we observed however that identical bands result in larger Nernst coefficient values. The Nernst coefficient peaks close to the middle of the bandgap where the Seebeck coefficient is zero. It increases linearly as the bandgap increases. However, we also obtained that the thermomagnetic power factor reduces as the bandgap increases.

We conclude that identical electron and hole bands that are anisotropic (in the crystallographic directions perpendicular to the magnetic field) with large s-parameters and zero or overlapping bands are the best candidates for good thermomagnetic materials.

References:

[1]   A. v. Ettingshausen and W. Nernst, *Ueber Das Auftreten Electromotorischer Kräfte in Metallplatten, Welche von Einem Wärmestrome Durchflossen Werden Und Sich Im Magnetischen Felde Befinden*, Ann. Der Phys. Und Chemie **265**, 343 (1886).

[2]   H. J. Goldsmid, *The Ettingshausen Figure of Merit of Bismuth and Bismuth - Antimony Alloys*, Br. J. Appl. Phys. **14**, 271 (1963).

[3]   E. H. Hall, *Measurement of the Four Magnetic Transverse Effects*, Phys. Rev. **26**, 820 (1925).

[4]   P. W. Bridgman, *The Connections between the Four Transverse Galvanomagnetic and Thermomagnetic Phenomena*, Phys. Rev. **24**, 644 (1924).

[5]   S. Dushman, *Electron Emission from Metals as a Function of Temperature*, Phys. Rev. **21**, 623 (1923).

[6]   J. Clayhold, *Nernst Effect in Anisotropic Metals*, Phys. Rev. B **54**, 6103 (1996).

[7]   V. D. Ky, *Planar Hall and Nernst Effect in Ferromagnetic Metals*, Phys. Status Solidi **22**, 729 (1967).

[8]   R. B. Horst, *Thermomagnetic Figure of Merit: Bismuth*, J. Appl. Phys. **34**, 3246 (1963).

[9]   M. E. Ertl, G. R. Pfister, and H. J. Goldsmid, *The Nernst Effect of Bi-Sb Alloys Related*

Content Size Dependence of the Magneto-Seebeck Effect in Bismuth-Antimony Alloys, Br. J. Appl. Physics, **14**, (1963).

[10] R. T. Delves, *Thermomagnetic Effects in Semiconductors and Semimetals*, Reports Prog. Phys. **28**, 249 (1965).

[11] D. Armitage and H. J. Goldsmid, *Magneto-Seebeck and Nernst Effects in Cadmium Arsenide*, J. Phys. C Solid State Phys. **2**, 2389 (1969).

[12] W. Williams, *Some Adiabatic and Isothermal Effects in Bismuth Telluride*, Proc. Phys. Soc. **73**, 739 (1959).

[13] M. K. Zhitinskaya, S. A. Nemov, and T. E. Svechnikova, *Effect of Inhomogeneities of Bi2T3 Crystals on the Transverse Nernst-Ettingshausen Effect*, Semiconductors **31**, 375 (1997).

[14] R. Mansfield and W. Williams, *The Electrical Properties of Bismuth Telluride*, Proc. Phys. Soc. **72**, 733 (1958).

[15] E. H. Putley, *Thermoelectric and Galvanomagnetic Effects in Lead Selenide and Telluride*, Proc. Phys. Soc. Sect. B **68**, 35 (1955).

[16] K. Behnia and H. Aubin, *Nernst Effect in Metals and Superconductors: A Review of Concepts and Experiments*, Reports Prog. Phys. **79**, 046502 (2016).

[17] E. H. Sondheimer and A. H. Wilson, *The Theory of the Galvanomagnetic and Thermomagnetic Effects in Metals*, Proc. R. Soc. London. Ser. A. Math. Phys. Sci. **193**, 484 (1948).

[18] V. Oganesyan and I. Ussishkin, *Nernst Effect, Quasiparticles, and d -Density Waves in Cuprates*, Phys. Rev. B **70**, 054503 (2004).

[19] A. E. Bowley, R. Delves, and H. J. Goldsmid, *Magnetothermal Resistance and Magnetothermoelectric Effects in Bismuth Telluride*, Proc. Phys. Soc. **72**, 401 (1958).

[20] E. H. Putley, *The Hall Coefficient, Electrical Conductivity and Magneto-Resistance Effect of Lead Sulphide, Selenide and Telluride*, Proc. Phys. Soc. Sect. B **68**, 22 (1955).

[21] I. M. TSidilḱovskiĭ, A. Tybulewicz, and H. J. Goldsmid, *Thermomagnetic Effects in Semiconductors* (Academic Press, New York, 1962).

[22] T. Ariga, M. Koyano, and A. Ishida, *Nernst Coefficient and Scattering Parameter in PbTe Films*, Phys. Status Solidi Basic Res. **249**, 1546 (2012).

[23] G. Mahan, *Good Thermoelectrics*, Solid-State Phys. **51**, 81 (1998).

[24] H. J. Goldsmid, *Introduction to Thermoelectricity*, Vol. 121 (Springer Series in

Materials Science, Berlin Heidelberg, 2010).

[25] M. Zebarjadi, K. Esfarjani, M. S. Dresselhaus, Z. F. Ren, and G. Chen, *Perspectives on Thermoelectrics: From Fundamentals to Device Applications*, Energy Environ. Sci. **5**, 5147 (2012).

[26] E. H. Sondheimer and A. H. Wilson, *The Theory of the Magneto-Resistance Effects in Metals*, Proc. R. Soc. London. Ser. A. Math. Phys. Sci. **190**, 435 (1947).

[27] N. F. MOTT, *The Modern Theory of Solids*, Nature **147**, 623 (1941).

[28] A. Sommerfeld and N. H. Frank, *The Statistical Theory of Thermoelectric, Galvano- and Thermomagnetic Phenomena in Metals*, Rev. Mod. Phys. **3**, 1 (1931).

[29] E. H. Putley, *Thermo- and Galvano-Magnetic Coefficients for Semiconductors*, Proc. Phys. Soc. Sect. B **65**, 991 (1952).

[30] P. J. Price, *Theory of Transport Effects in Semiconductors: The Nernst Coefficient, and Its Relation to Thermoelectric Power*, Phys. Rev. **102**, 1245 (1956).

[31] A. Einstein, *Über Die von Der Molekularkinetischen Theorie Der Wärme Geforderte Bewegung von in Ruhenden Flüssigkeiten Suspendierten Teilchen*, Ann. Phys. **322**, 549 (1905).

[32] R. Masuki, T. Nomoto, and R. Arita, *Origin of Anomalous Temperature Dependence of the Nernst Effect in Narrow-Gap Semiconductors*, Phys. Rev. B **103**, L041202 (2021).

[33] D. I. Pikulin, C. Y. Hou, and C. W. J. Beenakker, *Nernst Effect beyond the Relaxation-Time Approximation*, Phys. Rev. B **84**, 35133 (2011).

[34] R. Lundgren, P. Laurell, and G. A. Fiete, *Thermoelectric Properties of Weyl and Dirac Semimetals*, Phys. Rev. B **90**, 165115 (2014).

[35] G. Sharma, P. Goswami, and S. Tewari, *Nernst and Magnetothermal Conductivity in a Lattice Model of Weyl Fermions*, Phys. Rev. B **93**, 035116 (2016).

[36] G. Sharma, C. Moore, S. Saha, and S. Tewari, *Nernst Effect in Dirac and Inversion-Asymmetric Weyl Semimetals*, Phys. Rev. B **96**, 195119 (2017).

[37] S. Saha and S. Tewari, *Anomalous Nernst Effect in Type-II Weyl Semimetals*, Eur. Phys. J. B **91**, (2018).

[38] K. Das and A. Agarwal, *Berry Curvature Induced Thermopower in Type-I and Type-II Weyl Semimetals*, Phys. Rev. B **100**, 085406 (2019).

[39] M. N. Chernodub, A. Cortijo, and M. A. H. Vozmediano, *Generation of a Nernst Current from the Conformal Anomaly in Dirac and Weyl Semimetals*, Phys. Rev. Lett.

120, 206601 (2018).

[40] K. Das and A. Agarwal, *Thermal and Gravitational Chiral Anomaly Induced Magneto-Transport in Weyl Semimetals*, Phys. Rev. Res. **2**, 013088 (2020).

[41] M. Lundstrom, *Fundamentals of Carrier Transport*, 2nd ed. (Cambridge University Press, Cambridge, 2000).

[42] A. C. Smith, J. F. Janak, and R. B. Adler, *Electronic Conduction in Solids* (McGraw-Hill, 1967).

[43] H. Fieber, A. Nedeluha, and K. M. Koch, *Die Anomalie Der Galvano- Und Thermomagnetischen Transversaleffekte*, Zeirs. Fir PIlysik **131**, 143 (1952).

[44] N. H. March, B. V. Paranjape, and R. E. Robson, *Nernst, Ettingshausen and Righi-Leduc Phenomena in Relation to the Quantum Hall Effect in Two-Dimensional Electron Assemblies*, J. Phys. Chem. Solids **54**, 745 (1993).

[45] G. Moreau, *Sur Les Phénomènes Thermomagnétiques*, J. Phys. Théorique Appliquée **9**, 497 (1900).

[46] E. H. Hall and L. L. Campbell, *On the Electromagnetic and the Thermomagnetic Transverse and Longitudinal Effects in Soft Iron*, Proc. Am. Acad. Arts Sci. **46**, 625 (1911).

[47] M. S. Akhanda, S. E. Rezaei, K. Esfarjani, S. Krylyuk, A. V. Davydov, and M. Zebarjadi, *Thermomagnetic Properties of Bi2Te3 Single Crystal in the Temperature Range from 55 K to 380 K*, Phys. Rev. Mater. **5**, 015403 (2021).

[48] B. He, Y. Wang, M. Q. Arguilla, N. D. Cultrara, M. R. Scudder, J. E. Goldberger, W. Windl, and J. P. Heremans, *The Fermi Surface Geometrical Origin of Axis-Dependent Conduction Polarity in Layered Materials*, Nat. Mater. **18**, 568 (2019).

[49] V. A. Rowe and P. A. Schroeder, *Thermopower of Mg, Cd and Zn between 1.2° and 300°K*, J. Phys. Chem. Solids **31**, 1 (1970).

[50] A. Burkov and M. Vedernikov, *Anomalous Anisotropy of High Temperature of Thermo-Emf in Beryllium*, Fiz. Tverd. Tela **28**, 3737 (1988).

[51] Y. Tang, B. Cui, C. Zhou, and M. Grayson, *P × N-Type Transverse Thermoelectrics: A Novel Type of Thermal Management Material*, J. Electron. Mater. **44**, 2095 (2015).

[52] A. Burkov, M. Vedernikov, V. Elenskii, and G. Kovtun, *Anisotropy of Thermo-EMF and Electroconductivity of High Purity Rhenium*, Fiz. Tverd. Tela **28**, 785 (1986).

[53] C. Zhou, S. Birner, Y. Tang, K. Heinselman, and M. Grayson, *Driving Perpendicular Heat Flow: (P×n)-Type Transverse Thermoelectrics for Microscale and Cryogenic Peltier*

Cooling, Phys. Rev. Lett. **110**, (2013).

[54]   T. Aono, *The Nernst Effect of Bi-Sb Alloys*, Jpn. J. Appl. Phys. **9**, 761 (1970).